

**Supporting Information for:
Molecular Titanium Nitrides: Nucleophiles Unleashed**

Lauren N. Grant,[§] Balazs Pinter,[†] Takashi Kurogi,[§] Maria E. Carroll,[§] Gang Wu,[‡] Brian C. Manor,[§] Patrick J. Carroll[§] and Daniel J. Mindiola^{§,*}

[§]*Department of Chemistry, University of Pennsylvania, 231 South 34th Street, Philadelphia PA, 19104.*

[†]*Eenheid Algemene Chemie (ALGC), Vrije Universiteit Brussel (VUB), Pleinlaan 2, 1050, Brussels (Belgium).*

[‡]*Department of Chemistry, Queen's University, Kingston, Ontario, Canada K7L 3N6.*

Corresponding author: E-mail, mindiola@sas.upenn.edu

Table of Contents

A. NMR Data	S2-S9
B. Phosphonylimide LT NMR experiments	S10-S11
C. Computational Details	S11-S17
D. Crystallography Details	S16-S17
E. Solid state ¹⁵ N NMR Details	S18
F. References	S19-S20

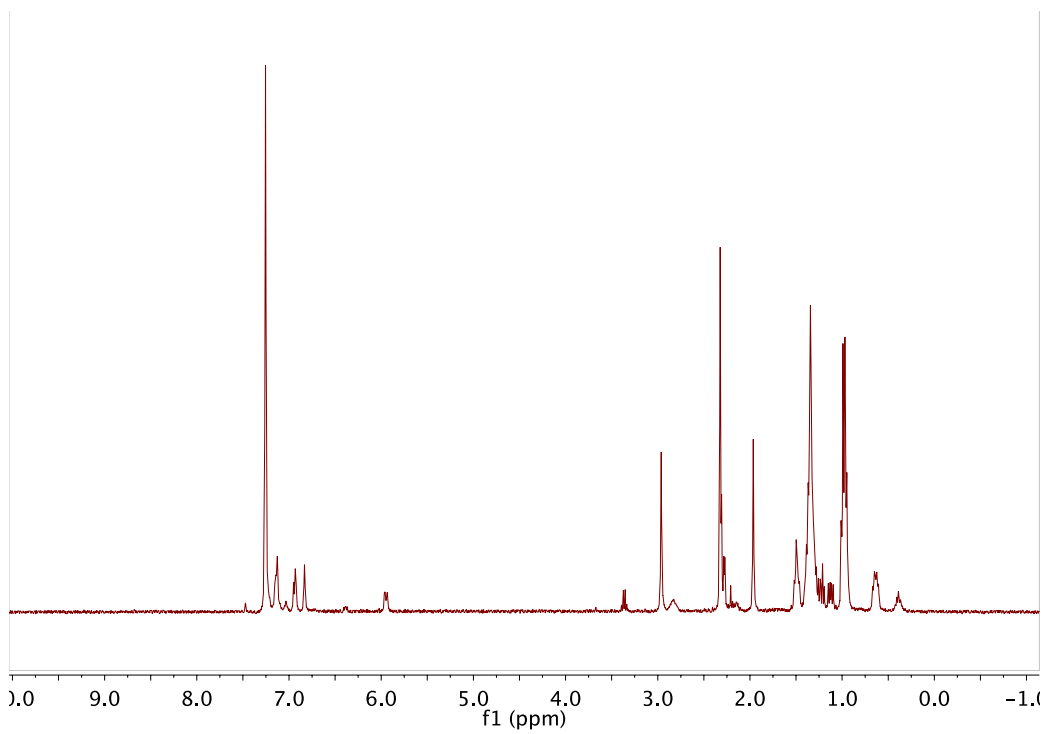


Figure S1: ^1H NMR Spectrum of **2** in C_6D_6 , 400 MHz, 300K

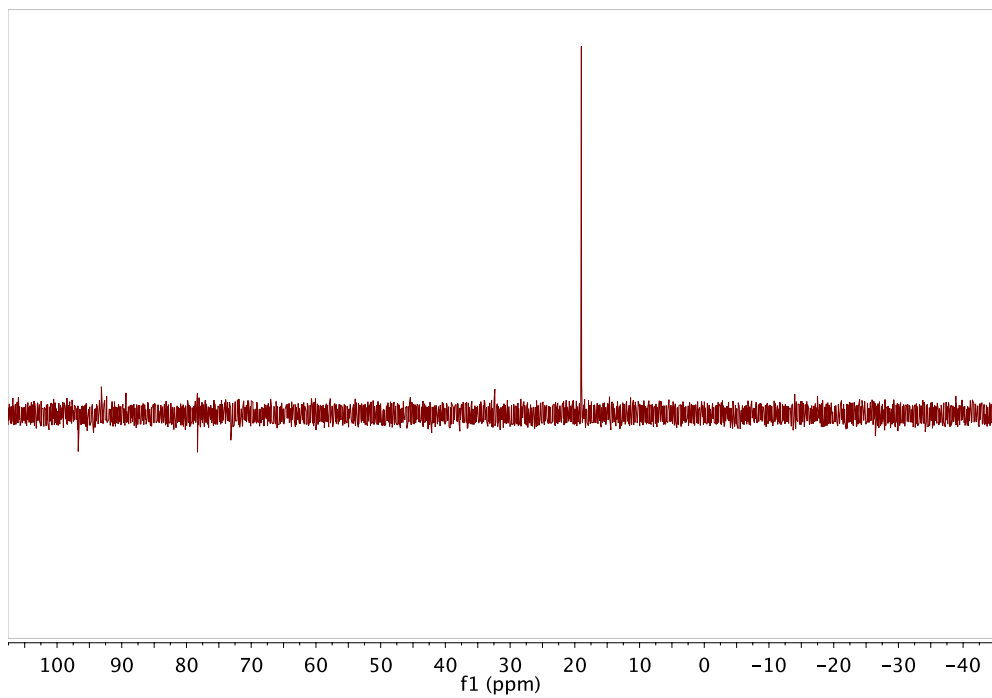


Figure S2: $^{31}\text{P}\{^1\text{H}\}$ NMR Spectrum of **2** in C_6D_6 , 162 MHz, 300K

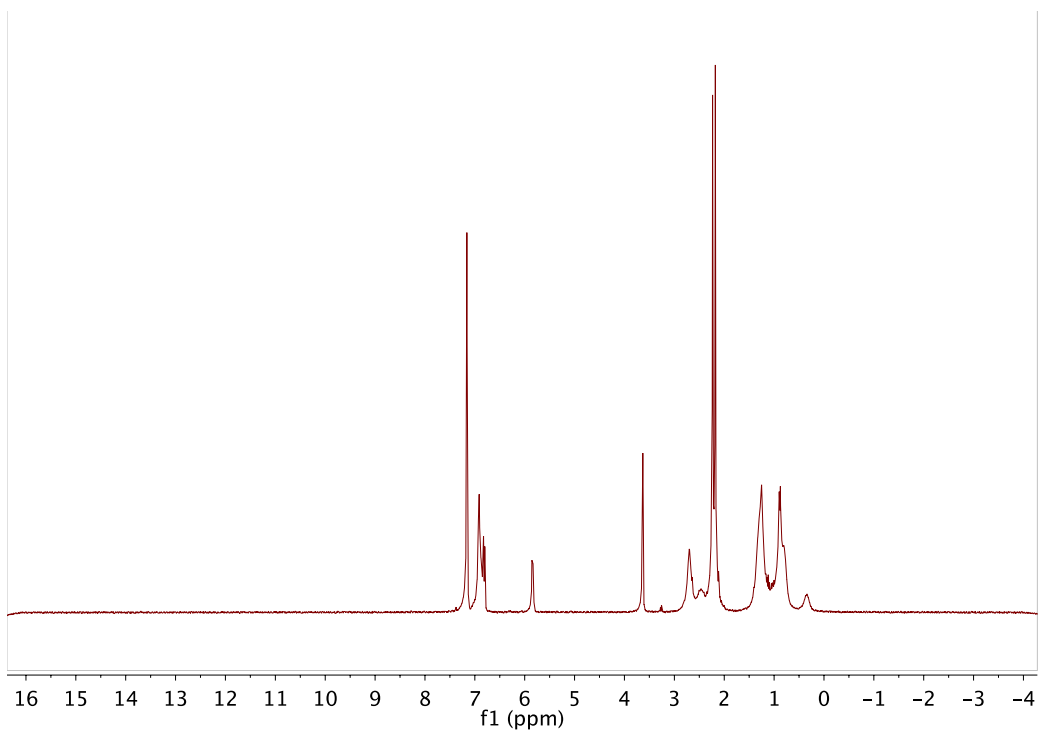


Figure S3: ^1H NMR Spectrum of **3** in C_6D_6 , 400 MHz, 300K

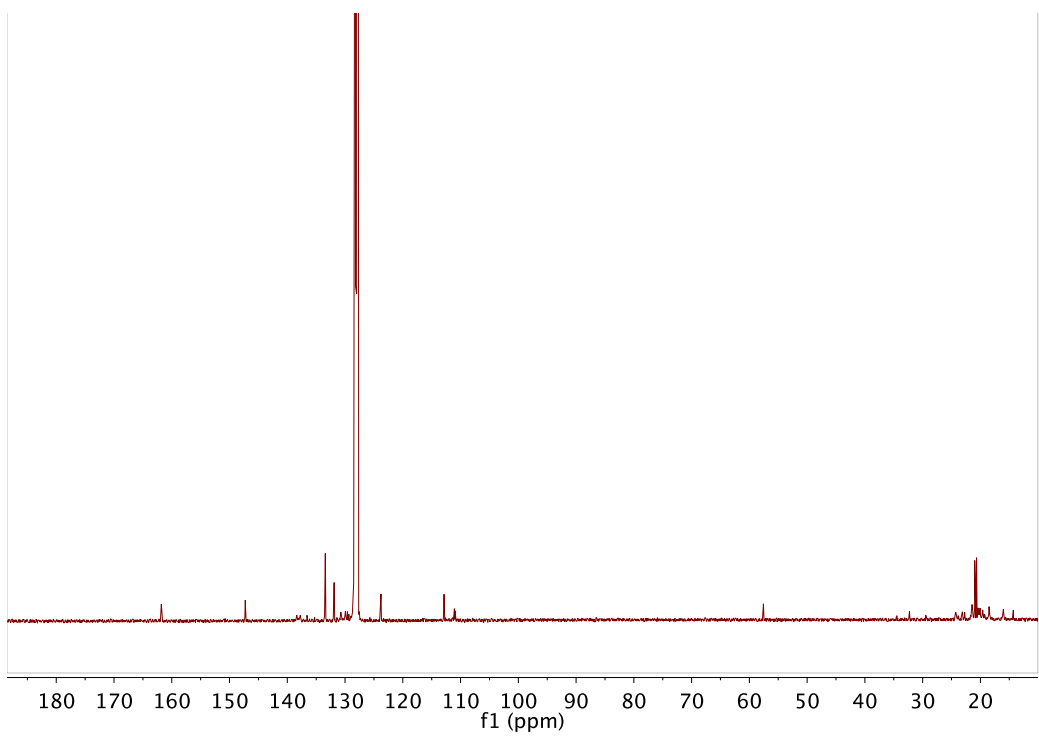


Figure S4: $^{13}\text{C}\{^1\text{H}\}$ NMR Spectrum of **3** in C_6D_6 , 125.8 MHz, 300K

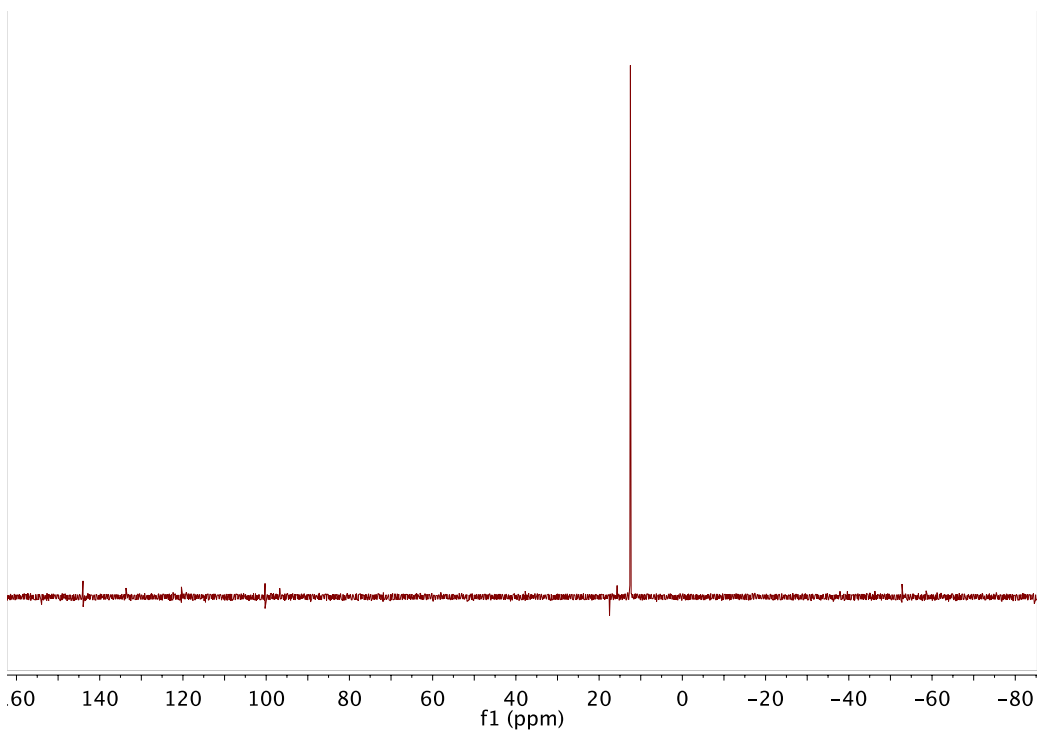


Figure S5: $^{31}\text{P}\{^1\text{H}\}$ NMR Spectrum of **3** in C_6D_6 , 162 MHz, 300K

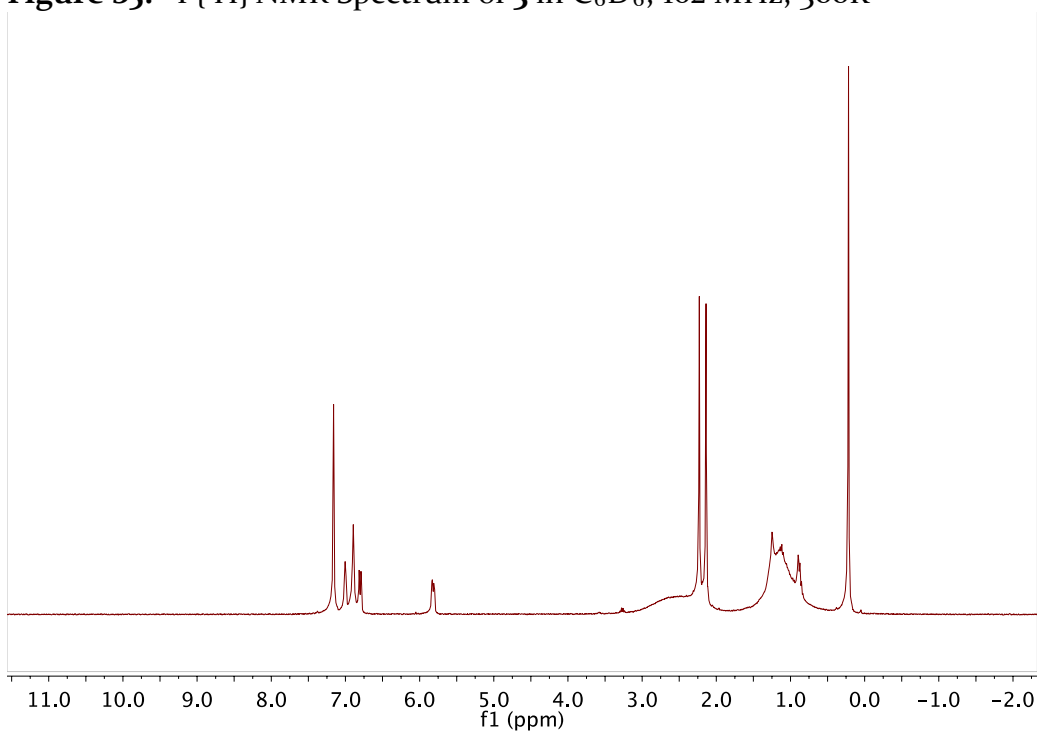


Figure S6: ^1H NMR Spectrum of **4** in C_6D_6 , 400 MHz, 300K

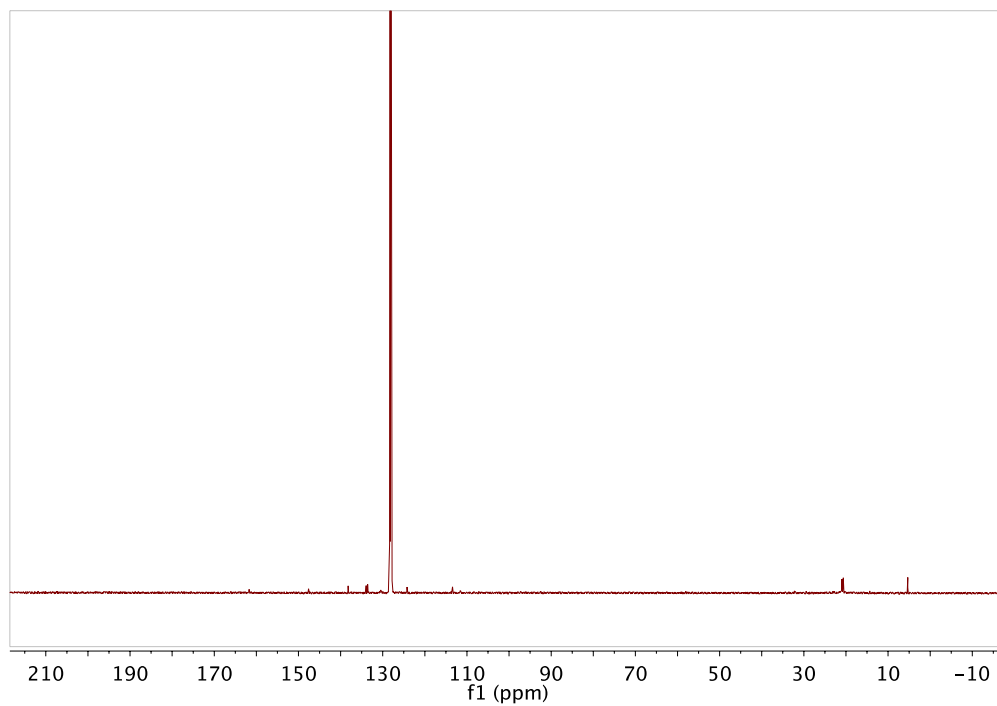


Figure S7: $^{13}\text{C}\{^1\text{H}\}$ NMR Spectrum of **4** in C_6D_6 , 125.8 MHz, 300K

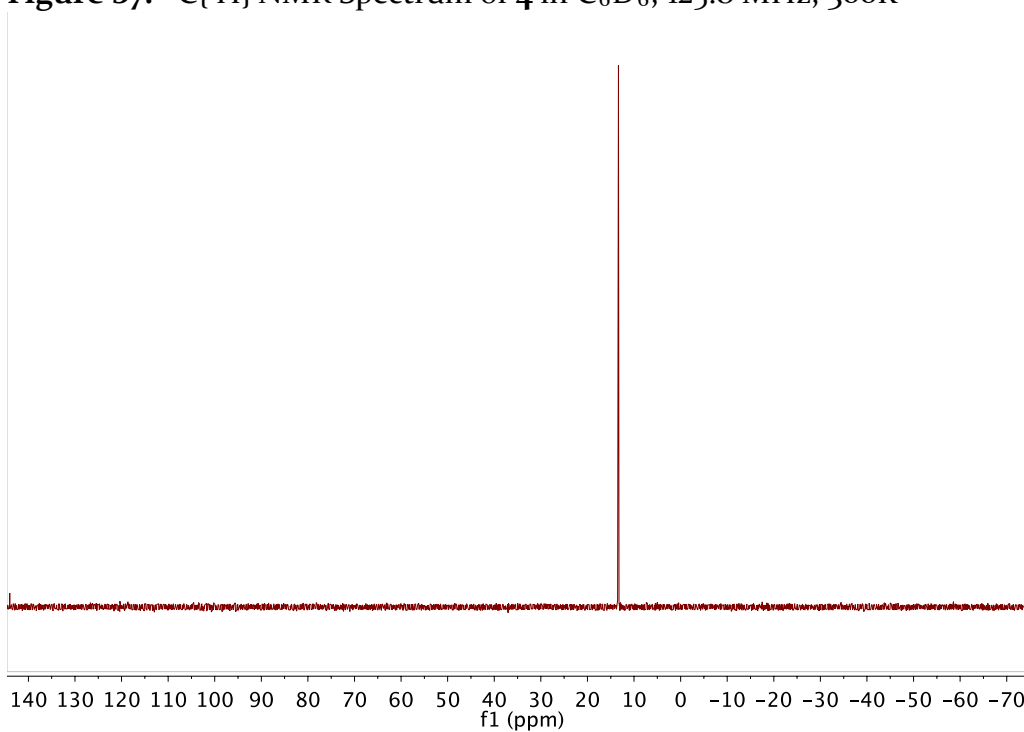


Figure S8: $^{31}\text{P}\{^1\text{H}\}$ NMR Spectrum of **4** in C_6D_6 , 162 MHz, 300K

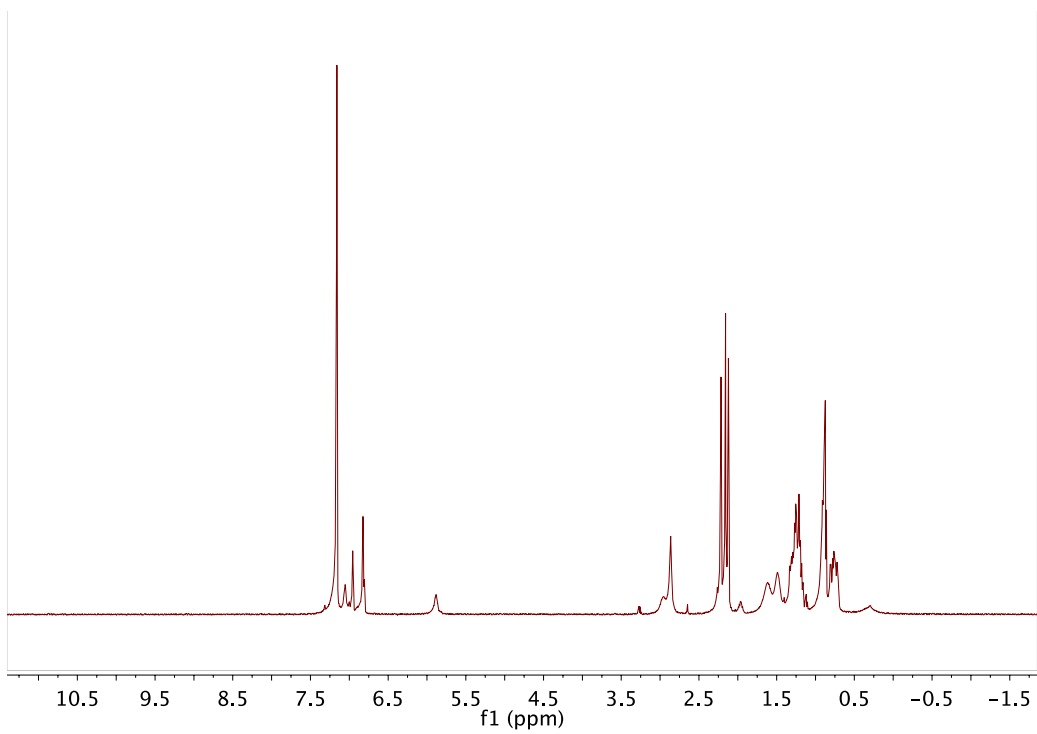


Figure S9: ^1H NMR Spectrum of **5** in C_6D_6 , 400 MHz, 300K

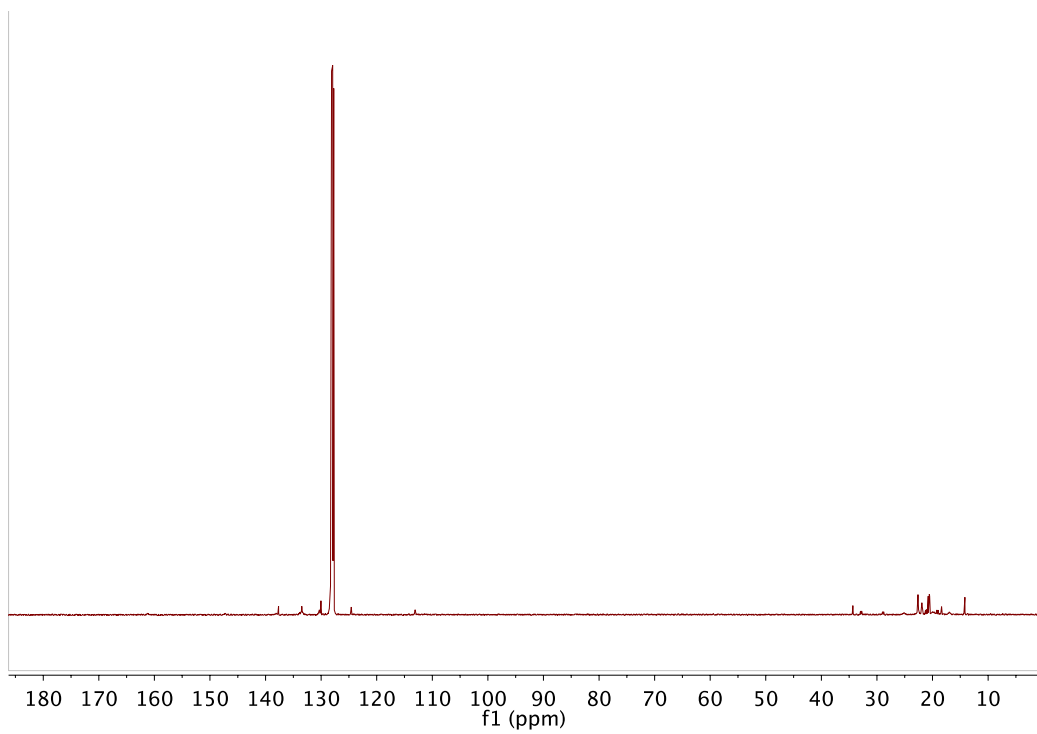


Figure S10: $^{13}\text{C}\{^1\text{H}\}$ NMR Spectrum of **5** in C_6D_6 , 125.8 MHz, 300K

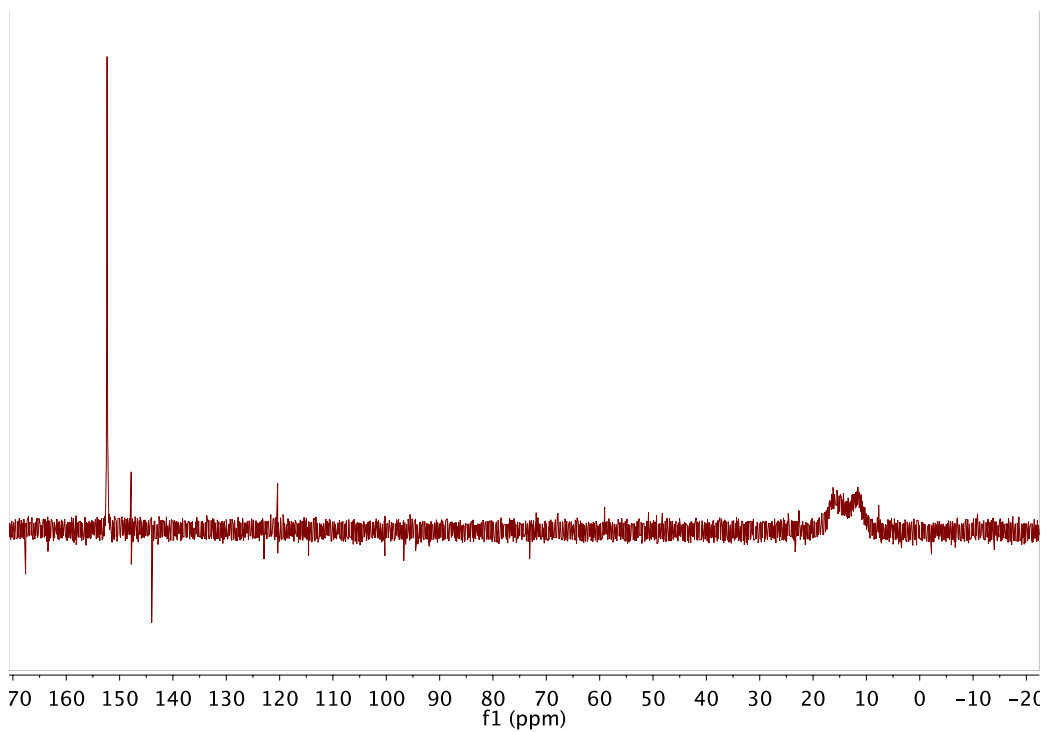


Figure S11: $^{31}\text{P}\{^1\text{H}\}$ NMR Spectrum of **5** in C_6D_6 , 162 MHz, 300K

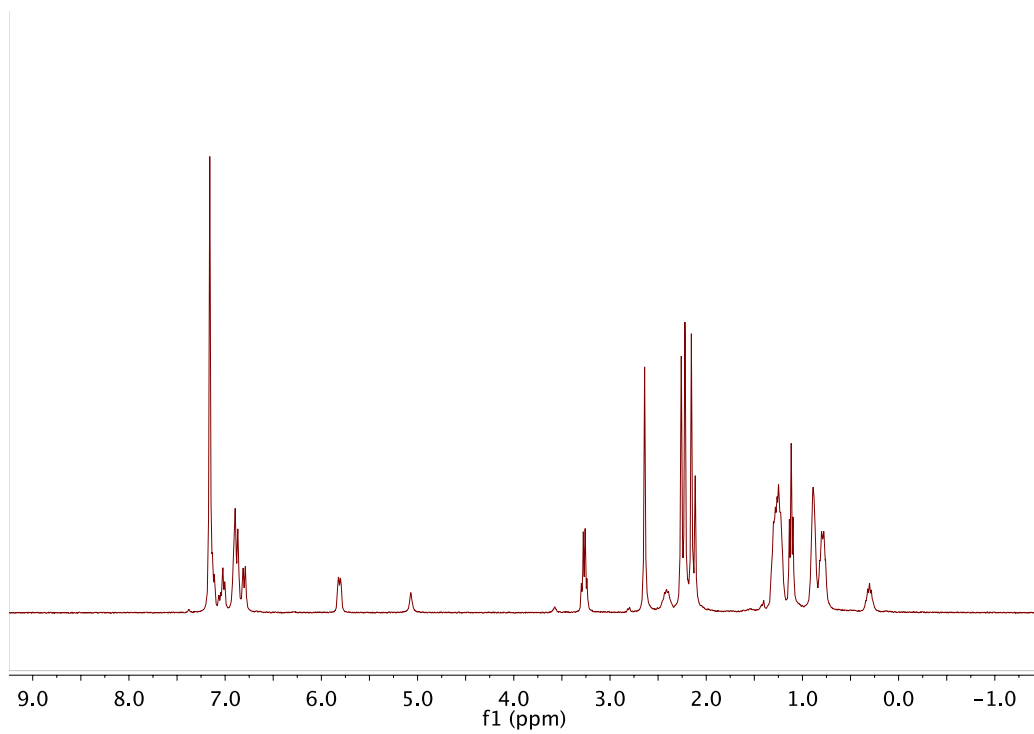


Figure S12: ^1H NMR Spectrum of **7** in C_6D_6 , 400 MHz, 300K

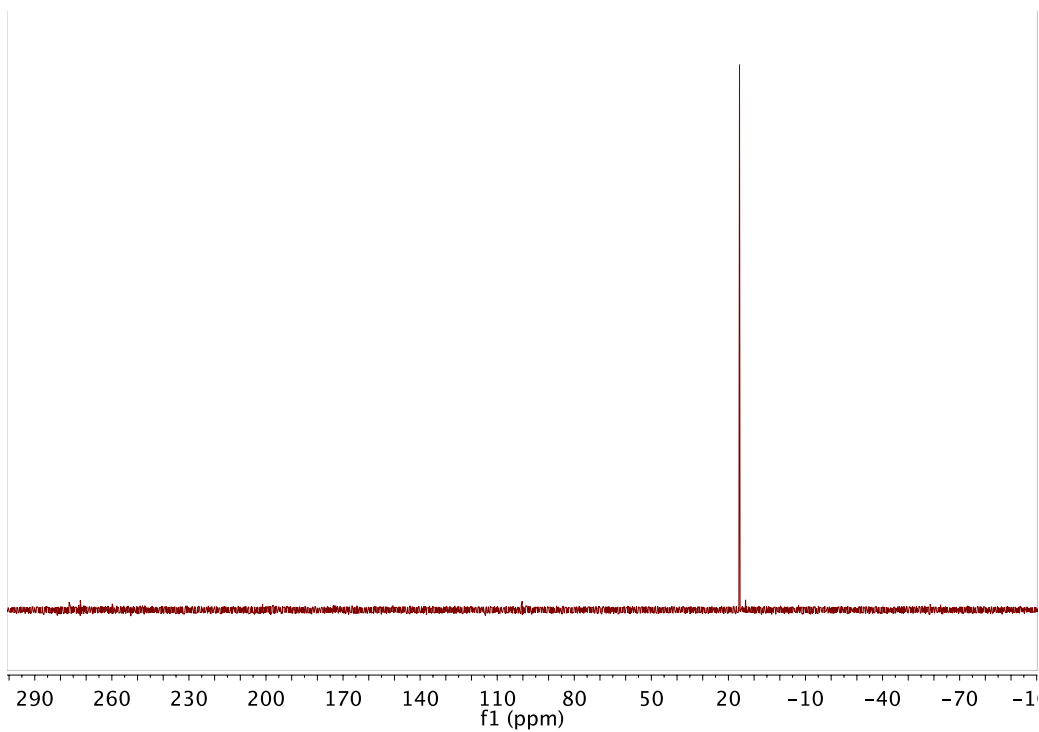


Figure S13: $^{31}\text{P}\{^1\text{H}\}$ NMR Spectrum of **7** in C_6D_6 , 162 MHz, 300K

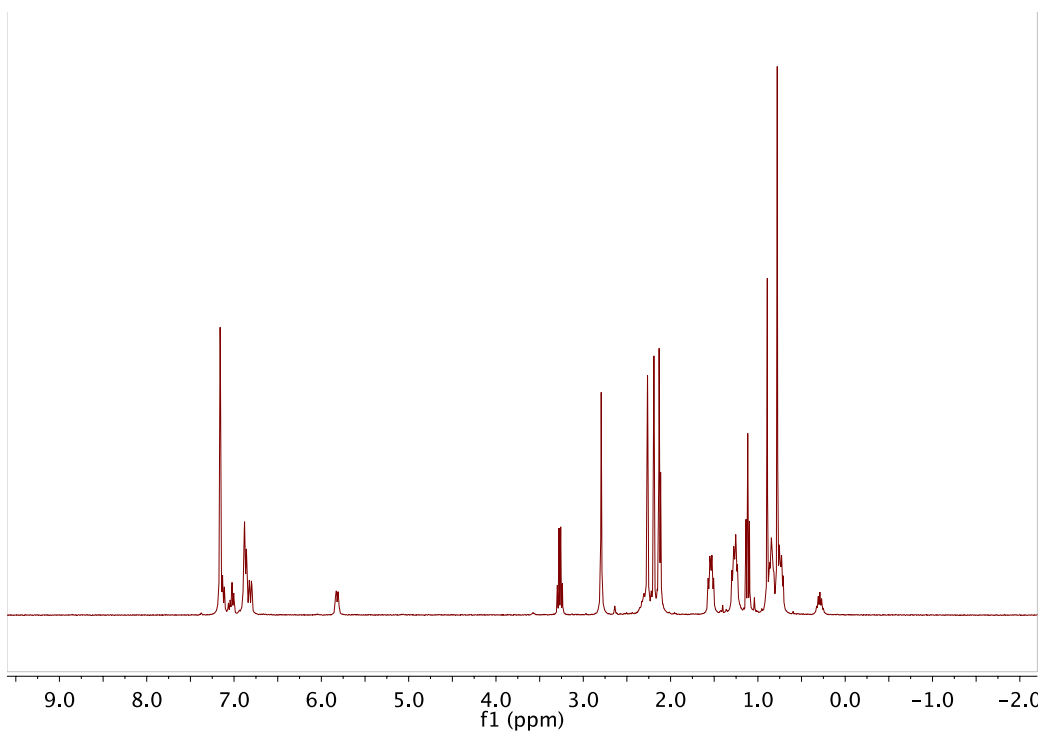


Figure S14: ^1H NMR Spectrum of **8** in C_6D_6 , 400 MHz, 300K

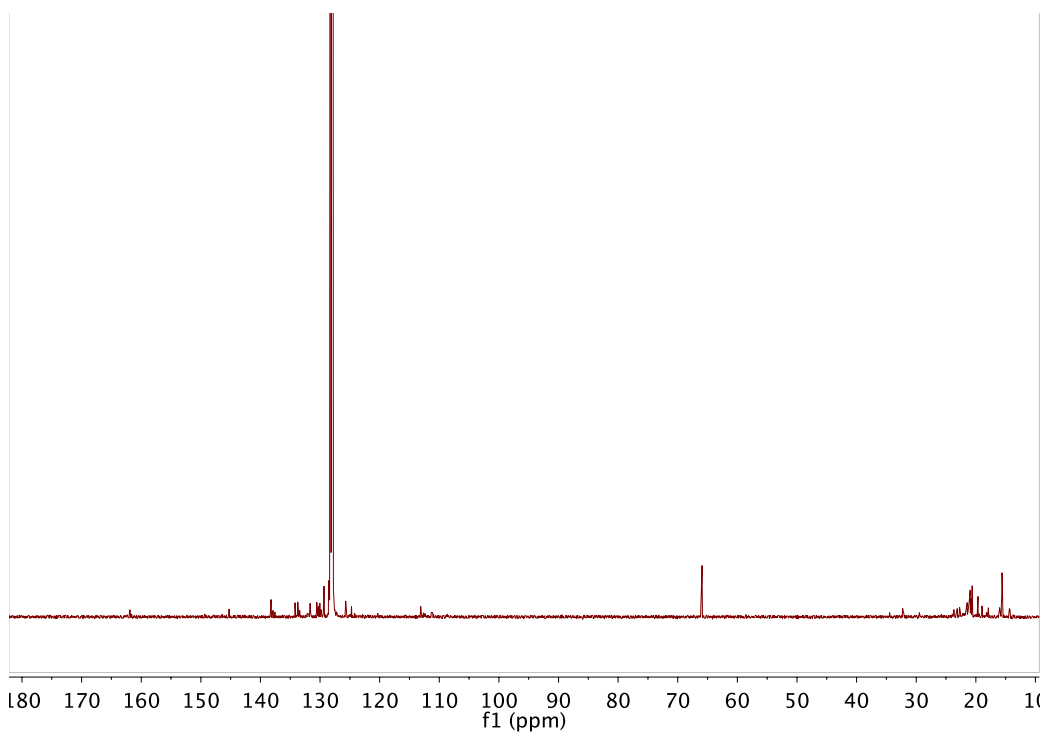


Figure S15: $^{13}\text{C}\{^1\text{H}\}$ NMR Spectrum of **8** in C_6D_6 , 125.8 MHz, 300K

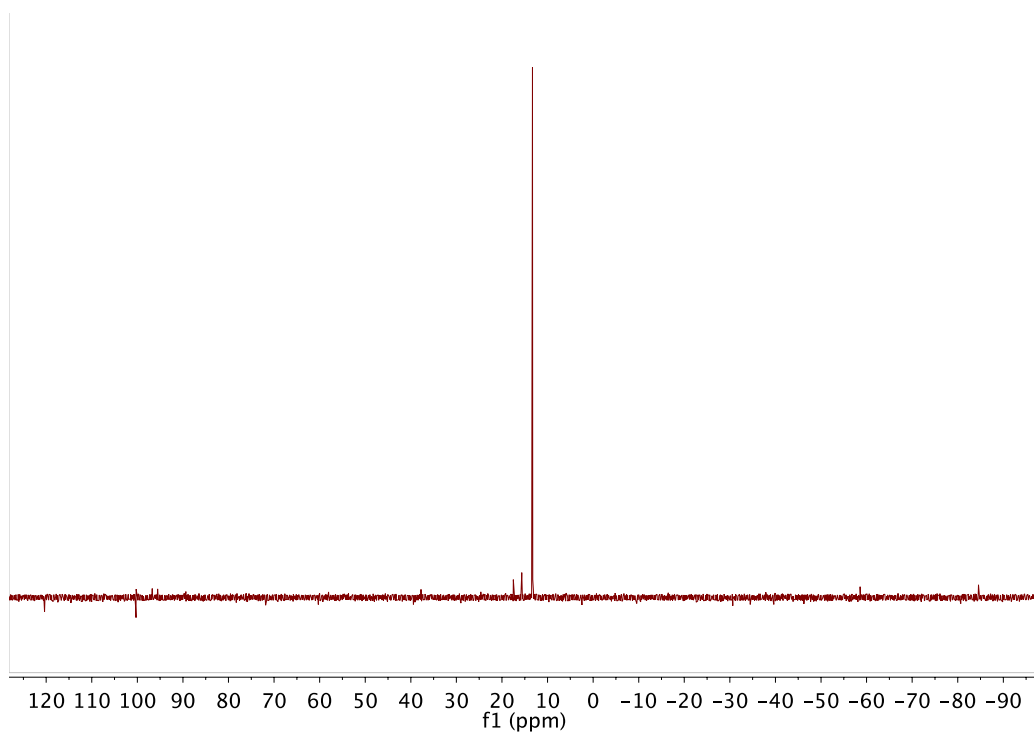


Figure S16: $^{31}\text{P}\{^1\text{H}\}$ NMR Spectrum of **8** in C_6D_6 , 162 MHz, 300K

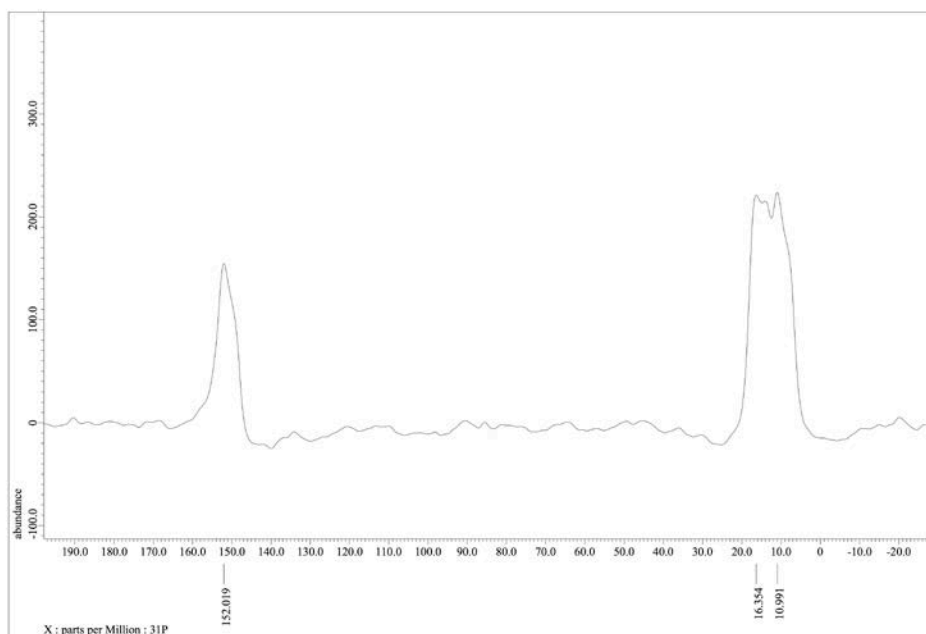


Figure S17: ^{31}P NMR Spectrum of **5** in C_7D_8 , 162 MHz, 265K

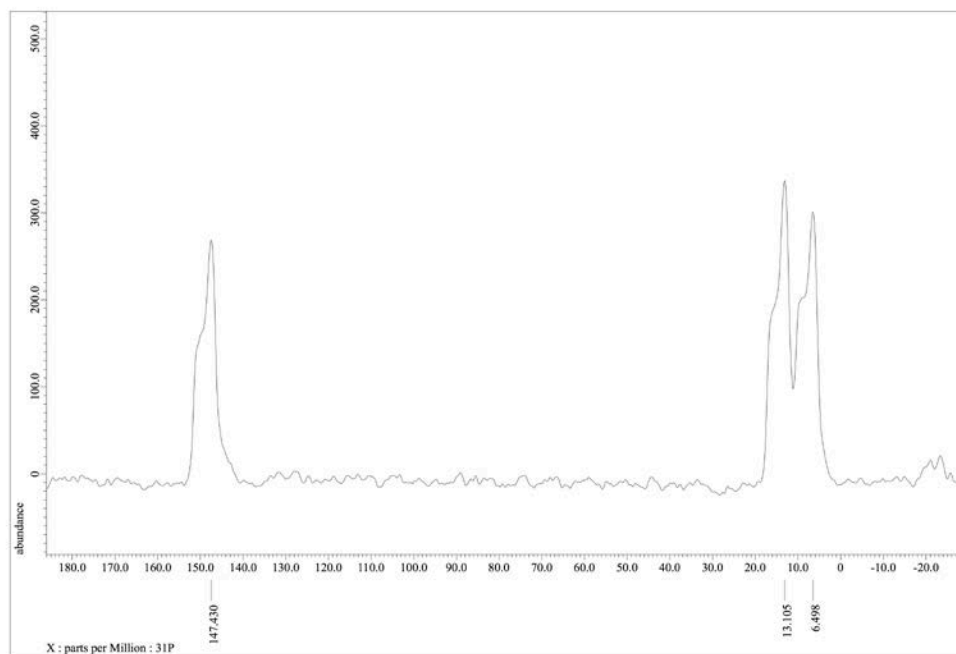


Figure S18: ^{31}P NMR Spectrum of **5** in C_7D_8 , 162 MHz, 219K

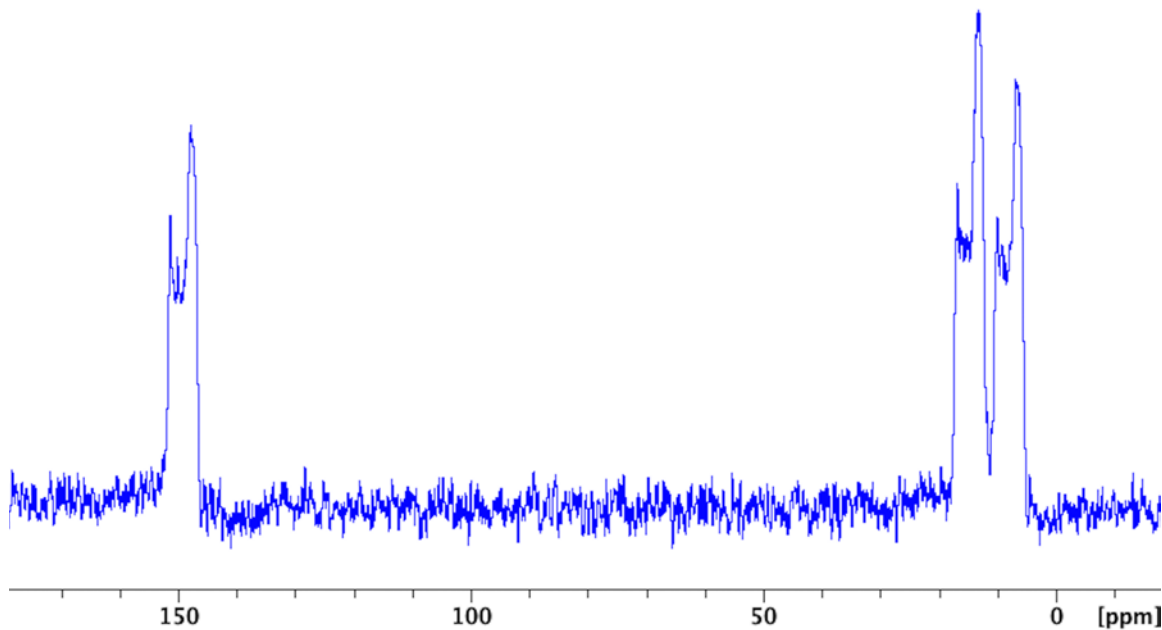


Figure S19. $^{31}\text{P}\{^1\text{H}\}$ NMR spectrum of **5**, taken at 219 K in C_7D_8 , 162 MHz.

Computational Details. All calculations were carried out using DFT as implemented in the ORCA program package¹. Final geometry optimizations were performed using the BLYP^{2,3} functional and the all-electron def2-TZVP(-f)-ZORA⁴ basis set in combination with the auxiliary basis set def2-TZV/J⁵. To accelerate geometry optimizations we used the resolution of the identity, R^6 , approximation. For these optimizations a tight convergence of the wavefunction was demanded on grid quality of Grid4 (also using SlowConv). The scalar relativistic zero'th order regular approximation (ZORA)⁷ was employed to take into account relativistic effects whereas to dispersion was considered using Grimme's D3 method in all ORCA calculations. Our experience with the optimizations of the investigated extended molecules (~ 200 atoms) is that the convergence to the equilibrium structure is much faster when optimizing in Cartesian coordinates (COPT). Finally, the above-described final geometry optimizations were started from pre-optimized structures obtained via a lower level of theory (BLYP/def2-SV(P), def2-SVP/J, ZORA, RI, d3, LooseSCF, Grid3).

We used the NMR module of ADF2013⁸ code to compute ^{15}N NMR chemical shifts on the equilibrium structures obtained via the protocol described above. The functional employed consisted of the local density approximation of Vosko, Wilk, and Nusair (LDA VWN)⁹ augmented with the nonlocal gradient correction PW91

from Perdew and Wang¹⁰. This functional has been shown to provide reliable chemical shift values even for heavy atom containing transition metal complexes¹¹. The full electron basis set TZVP was utilized in these calculations and relativistic corrections were applied using ZORA. The computed isotropic shielding values of complexes were referenced to that of ammonia modeled in the same way.

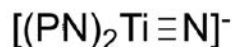
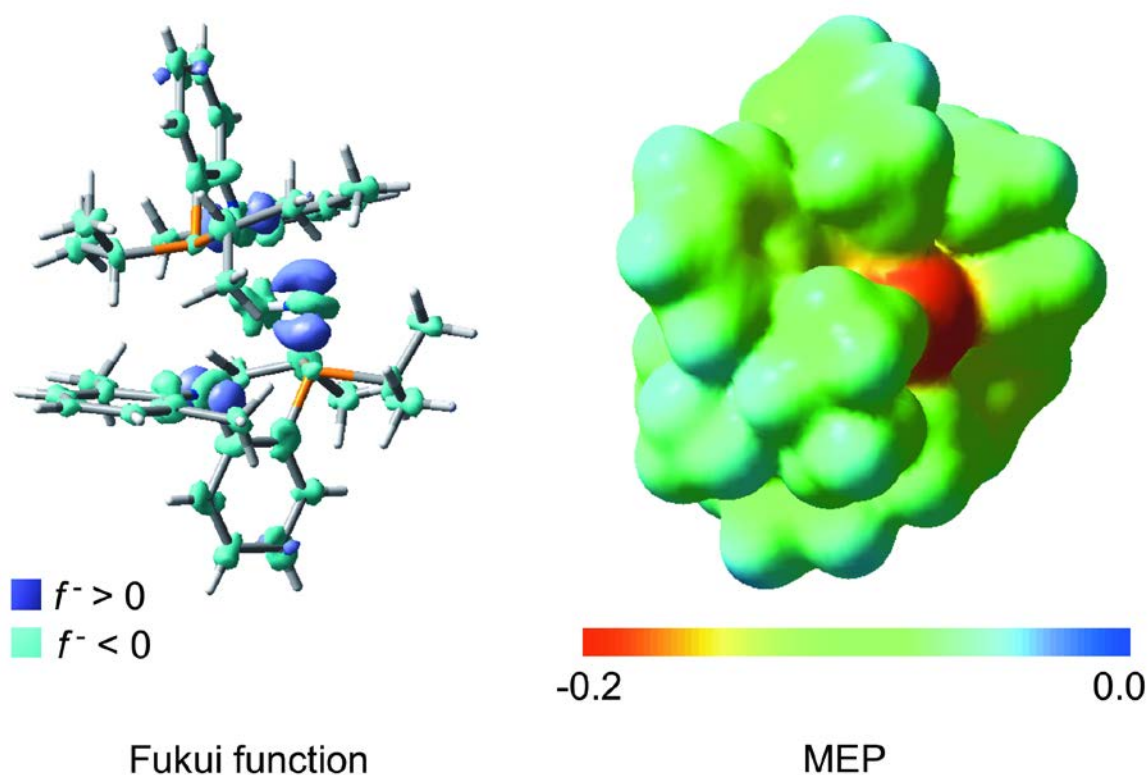


Figure S19. Nucleophilic Fukui function, f^- , and molecular electrostatic potential, MEP, for $[(\text{PN})_2\text{Ti}\equiv\text{N}]^-$ characterizing soft (purple regions) and hard (red sites) electrophilic reactivity of the titanium-nitride functionality, respectively,.

Crystallography Details. Suitable single crystals for X-ray analysis of **2-8** were placed on the end of a Cryoloop coated in NVH oil. The X-ray intensity data collection was carried out on a Bruker APEXII CCD area detector using graphite-monochromated Mo-K α radiation ($\lambda = 0.71073 \text{ \AA}$) at 100(1) K. Preliminary indexing was performed from a series of thirty-six 0.5° rotation frames with exposures of 10 seconds. Rotation frames were integrated using SAINT,¹² producing a listing of non-averaged F^2 and $\sigma(F^2)$ values which were then passed to the SHELXTL¹³ program package for further processing and structure solution. The intensity data were corrected for Lorentz and polarization effects and for absorption using SADABS.¹⁴ All calculations were performed using SHELXS¹⁵ and SHELXL.¹⁶ The structures were solved by Patterson and Fourier transform methods. All reflections were used during refinement. Non-hydrogen atoms were refined anisotropically and hydrogen atoms were refined using riding models with exception for **7**. For **4**, two crystallographically independent, but chemically equivalent molecules are present in the asymmetric unit. For **5**, ^iPr groups of NP^iPr_2 were disordered over two on the crystallographically special position. The thermal ellipsoids were fixed by SHELXL restraint commands,

DELU and SIMU. Disordered pentane molecule was located with 0.5 occupancies and a negative PART number, and refined with a rigid group model. For **6**, one site occupied by hexane was identified in the asymmetric unit. This site was considerably disordered and was treated by SQUEEZE as a diffuse contribution.^{17, 18} In the resulting void space, a contribution of 134 e⁻ per unit cell was found and taken to represent one hexane in the asymmetric unit, giving one pentane molecule for each Ti complex. For **7**, one site occupied by THF was identified in the asymmetric unit. This site was also treated by SQUEEZE as a diffuse contribution, resulting in a contribution of 186 e⁻ per unit cell to give one THF molecule for each Ti complex. This data was treated as a two-component crystal data. One component with 0.8 occupancies was refined as a terminally bound parent imide complex **7**. The hydrogen atom of the imide ligand was located from the difference map and refined isotropically. The second component was considerably an insertion product in which the imide ligand has inserted into the arm of the PN ligand. The phosphorus atom and corresponding ⁱPr groups were refined with 0.2 occupancies, but the hydrogen atom corresponding to the parent imide hydrogen in **7** could not be located from the difference map due to its low occupancy. These results were checked using the IUCR's CheckCIF routine. The alerts in the output are related to the disordered groups and crystal solvents.

Solid state ¹⁵N NMR Details. Solid-state ¹⁵N NMR spectra were recorded under the cross polarization (CP) magic-angle spinning (MAS) condition on a Bruker Avance-600 NMR spectrometer (14.1 T) operating at the ¹H and ¹⁵N Larmor frequencies of 600.17 and 60.81 MHz, respectively. The Hartmann-Hahn matching condition was established with a solid ¹⁵NH₄NO₃ sample. High-power ¹H decoupling (70 kHz) was applied during data acquisition. A 4-mm Bruker MAS probe was used with sample spinning frequencies between 5.0 and 14.5 kHz. A relaxation delay of 2 s and a contact time of 2 ms for CP were used. Powder samples were packed into a ZrO₂ rotor (4-mm o.d.) in a glove box. All ¹⁵N chemical shifts were referenced to that of NH₃(liq) ($\delta = 0$ ppm) by using solid ¹⁵NH₄NO₃ as a secondary ¹⁵N chemical shift reference ($\delta = 23.8$ ppm). Spectral simulations were performed using DMFit.¹⁹

References

- 1 F. Neese, ORCA—An ab initio, Density Functional and Semiempirical Program Package Version 3.0.1 (2013)
- 2 A. D. Becke, *Phys. Rev. A*, 1988, **38**, 3098.
- 3 C. T. Lee, W. T. Yang and R. G. Parr, *Phys. Rev. B*, 1988, **37**, 785.
- 4 D. A. Pantazis, X. Y. Chen, C. R. Landis and F. Neese, *J. Chem. Theory Comput.*, 2008, **4**, 908.
- 5 a) K. Eichkorn, F. Weigend, O. Treutler and R. Ahlrichs, *Theor. Chem. Acc.*, 1997, **97**, 119. b) K. Eichkorn, O. Treutler, H. Öhm, M. Häser and R. Ahlrichs, *Chem. Phys. Lett.*, 1995, **240**, 283.
- 6 K. Eichkorn, O. Treutler, H. Öhm, M. Häser and R. Ahlrichs, *Chem. Phys. Lett.*, 1995, **242**, 652.
- 7 a) E. van Lenthe, E. J. Baerends and J. G. Snijders, *J. Chem. Phys.*, 1993, **99**, 5648.; b) C. van Wullen, *J. Chem. Phys.*, 1998, **109**, 392.
- 8 E. J. Baerends, J. A., D. Bashford, A. Børces, F. M. Bickelhaupt, C. Bo, P. M. Boerrigter, L. Cavallo, D. P. Chong, L. Deng, R. M. Dickson, D. E. Ellis, M. van Faassen, M. Fan, T. H. Fischer, C. Fonseca Guerra, A. Ghysels, A. Giammona, S. J. A. van Gisbergen, A. W. Gotz, J. A. Groeneveld, O. V. Gritsenko, M. Grüning, F. E. Harris, P. Harris, P. van den Hoek, C. R. Jacob, H. Jacobsen, L. Jensen, G. van Kessel, F. Kootstra, M. V. Krykunov, E. van Lenthe, D. A. McCormack, A. Michalak, M. Mitoraj, J. Neugebauer, V. P. Nicu, L. Noodleman, V. P. O. Osinga, S. Patchkovskii, P. H. T. Philipsen, D. Post, C. C. Pye, W. Ravenek, J. I. Rodriguez, P. Ros, P. R. T. Schipper, G. Schreckenbach, M. Seth, J. G. Snijders, M. Solà, M. Swart, D. Swerhone, G. te Velde, P. Vernooijs, L. Versluis, L. Visscher, O. Visser, F. Wang, T. A. Wesolowski, E. M. van Wezenbeek, G. Wiesenekker, S. K. Wolff, T. K. Woo, A. L. Yakovlev and T. Ziegler, V. U. *ADF2013.01*, Amsterdam (The Netherlands).
- 9 S. H. Vosko, L. Wilk, Nusair, M. *Can. J. Phys.* 1980, **58**, 1200.
- 10 J. P. Perdew, J. A. Chevary, S. H. Vosko, K. A. Jackson, M. R. Pederson, D. J. Singh and C. Fiolhais, *Phys. Rev. B*, 1992, **46**, 6671.
- 11 M. Krykunov, T. Ziegler, E. van Lenthe, *J. Phys. Chem. A*, 2009, **113**, 11495 and references therein.
- 12 *SAINTE*; Bruker AXS Inc.: Madison, WI, USA. 2009.
- 13 *SHELXTL*; Bruker AXS Inc.: Madison, WI, USA, 2009.
- 14 G. M. Sheldrick, *SADABS*; University of Gottingen: Germany, 2007.
- 15 G. M. Sheldrick, *Acta Crystallogr.* 2008, **A64**, 112.
- 16 $R_1 = \Sigma ||F_o| - |F_c|| / \Sigma |F_o|$, $wR_2 = [\Sigma w(F_o^2 - F_c^2)^2 / \Sigma w(F_o^2)^2]^{1/2}$, $GOF = [\Sigma w(F_o^2 - F_c^2)^2 / (n - p)]^{1/2}$; where n = the number of reflections and p = the number of

parameters refined.

17 A. L. Spek, *Acta Crystallogr.* 2009, **D65**, 148.

18 P. van der Sluis and A. L. Spek, *Acta Crystallogr.* 1990, **A46**, 194.

19 D. Massiot, F. Fayon, M. Capron, I. King, S. Le Calvé, B. Alonso, J.-O. Durand, B. Bujoli, Z. Gan, G. Hoatson, Modelling one- and two-dimensional solid-state NMR spectra. *Magn. Reson. Chem.*, 2002, **40**, 70-76.